ORIGINAL ARTICLE

Individualized volume CT dose index determined by cross-sectional area and mean density of the body to achieve uniform image noise of contrast-enhanced pediatric chest CT obtained at variable kV levels and with combined tube current modulation

Hyun Woo Goo

Abstract

Background A practical body-size adaptive protocol providing uniform image noise at various kV levels is not available for pediatric CT.

Objective To develop a practical contrast-enhanced pediatric chest CT protocol providing uniform image noise by using an individualized volume CT dose index (CTDIvol) determined by the cross-sectional area and density of the body at variable kV levels and with combined tube current modulation.

Materials and methods A total of 137 patients (mean age, 7.6 years) underwent contrast-enhanced pediatric chest CT based on body weight. From the CTDIvol, image noise, and area and mean density of the cross-section at the lung base in the weight-based group, the best fit equation was estimated with a very high correlation coefficient ($\gamma^2 = 0.86$, $P<0.001$). For the next study, 177 patients (mean age, 7.9 years; the CTDIvol group) underwent contrast-enhanced pediatric chest CT with the CTDIvol determined individually by the best fit equation. CTDIvol values on the dose report after CT scanning, noise differences from the target noise, areas, and mean densities were compared between these two groups.

Results The CTDIvol values (mean±standard deviation, 1.6±0.7 mGy) and the noise differences from the target noise (1.1±0.9 HU) of the CTDIvol group were significantly lower than those of the weight-based group (2.0±1.0 mGy,

1.8±1.4 HU) ($P<0.001$). In contrast, no statistically significant difference was found in area (317.0±136.8 cm^2 vs. 326.3±124.8 cm^2), mean density (−212.9±53.1 HU vs. −221.1±56.3 HU), and image noise (13.8±2.3 vs. 13.6±1.7 HU) between the weight-based and the CTDIvol groups ($P>0.05$).

Conclusion Contrast-enhanced pediatric chest CT with the CTDIvol determined individually by the cross-sectional area and density of the body provides more uniform noise and better dose adaptation to body habitus than does weight-based CT at variable kV levels and with combined tube current modulation.

Keywords Chest CT in children · Image quality · Radiation dose · Body weight · Cross-sectional area · Body density

Introduction

A body size-adaptive pediatric CT protocol should be used to minimize the adverse effects of radiation exposure [1, 2]. Of such protocols, a body weight-based CT protocol is most commonly used as it is easy to use [3, 4]. However, CT protocols based on cross-sectional dimensions such as diameter, area, and circumference have been advocated for better dose adaptation to body habitus than the weight-based CT protocol [5–11]. Patient body diameter derived from the attenuation value on a scout image has been used in some studies [10, 11]. In one study [12], uniform image quality of coronary CT angiography could be achieved by individual tube current modulation using the image noise measured on unenhanced CT images for calcium scoring. However, the method cannot be applied to the single-phase

H. W. Goo (✉)
Department of Radiology and Research Institute of Radiology,
Asan Medical Center, University of Ulsan College of Medicine,
Asanbyeongwon-gil 86, Songpa-gu,
Seoul 138-736, Korea
e-mail: hwgoo@amc.seoul.kr

CT scanning that is typical for contrast-enhanced pediatric chest CT.

Tube current modulation is a very useful dose-saving technique based on patient-specific attenuation because it can substantially reduce CT dose without degrading image quality [13, 14]. However, this technique needs to be adjusted to body size to ensure dose optimization, and the user must define appropriate reference mAs or noise index reflecting each patient size before CT scanning [15]. Otherwise, inappropriate under- or over-exposure may occur in slim or obese patients. In addition, it is noteworthy that current tube current modulation techniques do not include tube potential adaptation, which is important for a body size-adaptive pediatric body CT protocol using variable kV levels [16]. In fact, there is no clear guideline for the use of tube current modulation at 80–100 kV for a given patient size, anatomical region, and clinical indication.

The importance of establishing a body size-adaptive pediatric CT protocol, particularly based on cross-sectional dimensions, has been emphasized. In reality however, a practical body size-adaptive pediatric CT protocol has not been reported. To be practical, patient body size parameters should be easily obtainable prior to CT scanning, and CT dose parameters based on the body size parameters should be continuous rather than ordinal as in a CT dose table. The method also can provide CT dose parameters and uniform image noise at different kV levels, as variable kV levels are used commonly in pediatric body CT [3]. Therefore, the aim of this study was to develop a practical contrast-enhanced pediatric chest CT protocol providing uniform image noise, which was adjusted individually by patient factors, by using individualized volume CT dose index (CTDIvol = CTDIw/pitch factor) determined by the cross-sectional area and mean density of the body at variable kV levels and with combined tube current modulation.

Materials and methods

This study was approved by our institutional review board and the requirement for written informed consent was waived.

Body weight-based contrast-enhanced chest CT

Between September 2007 and January 2008, 137 patients younger than 18 years of age (mean age, 7.6 years; range, 3 months–17 years) underwent contrast-enhanced pediatric chest CT based on our weight-based protocol (Table 1). In the weight-based protocol, radiation dose was adjusted empirically to the reference noise level (the standard deviation of the CT numbers measured in the descending thoracic aorta) of diagnostic pediatric chest CT images, being in the range of 12.0–15.5, higher for larger patients. This group was assigned to the weight-based group. Contrast-enhanced chest CT examinations performed during the same period were excluded if the contrast enhancement measured in the descending aorta was below 250 HU or above 350 HU. Chest spiral CT using a 16-slice CT scanner (Somatom Sensation 16; Siemens Medical Solutions, Forchheim, Germany) was obtained with 16×1.5-mm collimation, 1.0 pitch, and 0.375-s gantry rotation time after intravenous administration of iodinated contrast agent (1.2 ml/kg; Iomeron 300, 300 mg I/ml; Bracco Imaging, Milan, Italy) followed by saline chaser using a dual-head power injector at an injection rate (0.3–3.0 ml/s) adjusted to a fixed injection

Table 1 Body weight-based chest computed tomography (CT) protocol (n=137). Data are described by mean±standard deviation if applicable. The numbers in parenthesis in the column of the CTDIvol represent the range of values

Body weight	Area (cm^2)	Density (HU)	kV	Effective mAs	Reference mAs	Reconstructed slice thickness (mm)	CTDIvol (mGy)[a]	Effective dose (mSv)	Image noise
< 5.0 kg (n=1)	101	−194	80	40	37	3.0	1.1	0.9	9
5.0–9.9 kg (n=11)	161±16	−180±51	80	50	45±10	4.0	1.2±0.3 (0.8–1.6)	1.1±0.4	12±3
10.0–19.9 kg (n=44)	214±27	−193±38	80	65	46±7	4.0	1.4±0.2 (1.2–2.2)	1.1±0.2	14±2
20.0–39.9 kg (n=40)	299±53	−205±55	80	90	47±7	5.0	1.8±0.1 (1.3–1.9)	1.2±0.3	14±2
40.0–59.9 kg (n=31)	454±60	−261±44	100	65	23±3	5.0	2.6±0.2	2.1±0.4	14±2
60.0–69.9 kg (n=5)	555±32	−233±30	100	100	33±7	5.0	4.5±0.9 (3.9–6.2)	2.6±1.5	13±2
> 70.0 kg (n=5)	667±82	−204±56	120	75	20±2	5.0	5.4±0.3 (5.0–5.7)	3.5±1.1	14±4

[a] CTDIvol values were based on a 32-cm CTDI phantom. To estimate dose length product (DLP, CTDIvol × scan range [cm])-based effective dose, conversion factors derived from a 16-cm CTDI phantom were used. Therefore, CTDIvol values (e.g., 2.0 mGy) based on a 32-cm CTDI phantom were multiplied by a factor of two to obtain CTDIvol values (e.g., 4.0 mGy) based on a 16-cm CTDI phantom

time (30 s) of contrast agent. A bolus tracking technique was used to determine a scan delay. For bolus tracking, an axial scan with 80 kV and 25 mAs was performed at the basal lung region (Fig. 1). This axial CT image was used for measurement of the cross-sectional area and its mean density by placing a region of interest (ROI) big enough to include the entire scanned cross-section (Fig. 1). Then, a round ROI was placed in the descending aorta to determine an optimal scan delay on the same axial CT image with a density threshold of 150 HU, a monitoring delay of 15 s, and a scan delay after bolus tracking of 15 s. Spiral CT scanning from the adrenal gland region to the supraclavicular region was acquired in a caudocranial direction to minimize perivenous artifacts. Combined tube current modulation (CARE Dose 4D; Siemens Medical Solutions), i.e., a combined dose-saving technique of angular and z-axis tube current modulations based on attenuation profiles of patient body obtained from actual CT projection data and scout data, was used. Axial CT images were reconstructed using a medium-smooth kernel (B30f) with 3- to 5-mm weight-adjusted reconstructed slice thickness (Table 1). CTDIvol values displayed on the dose report after finishing CT scanning were recorded. These CTDIvol values were based on a 32-cm CTDI phantom. Children younger than 5 years of age were sedated with oral chloral hydrate. Intravenous injection of midazolam and/or ketamine was added if necessary. General anesthesia or controlled ventilation was not used. Thus, all sedated children were free-breathing during the CT examination.

To measure the aortic enhancement (mean CT density) and the image noise (standard deviation of mean CT density), a rectangular ROI with approximately 50% of the aortic diameter was placed in the center of the descending thoracic aorta at three levels: the carina, the aortic valve, and the mid-ventricle on axial CT images reconstructed with 3- to 5-mm thickness. Three measured values were averaged for data analysis. As mentioned previously, the measured aortic enhancement of each CT examination had to be in the range of 250–350 HU to be included in this study.

Development of the best fit equation

Using the CTDIvol, image noise, cross-sectional area, and its mean density measured in the weight-based group, the equation of best fit was estimated on the basis of the following standard formula [12]:

$$CTDIvol \times \sigma^2 \propto \exp(\mu \times D)$$

where σ is image noise, exp is the exponential function, μ is the linear attenuation coefficient, and D the body diameter.

Curve estimation regression analysis was used to obtain the best fit equation, in which the mean density and the cross-sectional area were used as alternatives of the linear attenuation coefficient and the body diameter, respectively, in order to make the proposed formula practical for clinical use. Regarding image noise, which would be influenced considerably by the different slice thicknesses (3–5 mm) and kV levels (80–120 kV), it was tested whether either the square of the image noise or the image noise showed a higher correlation coefficient. Among various curve models, including linear, power, exponential, and logistic models, the linear model showed the highest correlation coefficient. The best fit equation using the image noise showed a higher correlation coefficient (R^2=0.86, $P<0.001$)
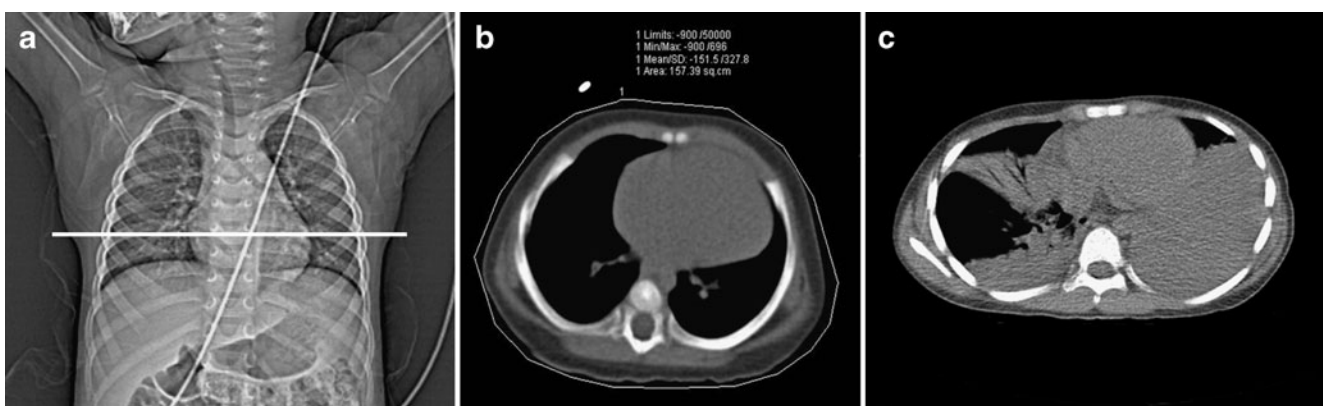

Fig. 1 The method of measurement of the area and its mean density of the lower thoracic cross-section. **a** Scout image shows the location of the single axial slice at the basal lung region for the measurements as well as bolus tracking for contrast-enhanced chest CT. **b** A region of interest is placed to include the entire thoracic cross-section on the axial CT image. To exclude the air outside the patient, the lower limit of CT density for the region of interest is set to −900 HU. The cross-sectional area and its mean density of the patient are then given instantaneously to be 157.39 cm^2 and −151.5 HU, respectively. **c** In a 9-year-old girl with pneumonia and pleural effusion, the mean density measured on the axial CT image was −79.6 HU, which resulted in an increase in the CTDIvol value of approximately 18.5% calculated by using the best fit equation

(Fig. 2) than that using the square of the image noise (R^2= 0.53, $P<0.001$). Therefore, the former equation was used to develop the best fit equation for the new CT protocol:

$$CTDIvol = \exp(0.003 \times A + 0.001 \times D_{400} + 2.2)/\sigma$$

where exp was the exponential function, D_{400} was the sum of the measured mean density (HU) and 400 HU (400 HU was added to the mean density in order to get a positive number), and σ was the measured image noise. The cross-sectional area, or its mean density, was correlated separately with the logarithm of a product of the CTDIvol value and the image noise by using the linear regression model (Fig. 2). The R^2 values for the cross-sectional area and its mean density were 0.85 ($P<0.001$) and 0.04 ($P=0.01$), respectively.

Contrast-enhanced chest CT using the new protocol

For the next part of the study, 177 patients younger than 18 years of age (mean age, 7.9 years; range, 2 months–17 years) underwent contrast-enhanced pediatric chest CT with individualized CTDIvol values between September 2008 and November 2009. This group was assigned to the CDTIvol group. Contrast-enhanced chest CT examinations performed during the same period were excluded if the contrast enhancement measured in the descending aorta was below 250 HU or above 350 HU. These excluded chest CT examinations were collected separately to evaluate the relationship between the degree of aortic enhancement and CT image noise. For each chest CT examination, a CTDIvol value was calculated from the measured cross-sectional area and its mean density using the best fit equation. Depending on the measured cross-sectional area, kV level and slice thickness were then determined (Table 2). Finally, the effective mAs value was adjusted to meet the calculated CTDIvol value. The other image acquisition parameters and intravenous injection protocol were identical to those in the weight-based group. Combined tube current modulation (CARE Dose 4D; Siemens Medical Solutions) was also used. CTDIvol and reference mAs values displayed on the dose report after finishing CT scanning were recorded.

Data analysis

Patient age, aortic enhancement, cross-sectional area, its mean density, and CTDIvol were compared between the two groups. In addition, image noise and aortic noise variance from the target image noise were compared between the two groups. In both groups, the target image noise was calculated by the measured cross-sectional area using the following formula with a power regression model:

$$\sigma_t = \exp\{1.8 + (0.1 \times Ln[A])\}$$

where σ_t is the target image noise, exp is the exponential function, Ln is the natural logarithm, and A the measured cross-sectional area.

In the weight-based group and the CTDIvol group, the cross-sectional area, its mean density, and reference mAs were correlated with the image noise at 80 kV (n=96 and 123) and 100 kV (n=36 and 51). Only five and three chest CT examinations were performed at 120 kV and, therefore, those cases were excluded from the linear correlation analysis. In spite of the low R^2 value (0.04) for the mean density in the linear regression analysis, a potential effect of the considerably high mean density on the resultant CTDIvol in cases showing thoracic pathologies such as consolidation, atelectasis, pleural effusion, cardiomegaly, and chest mass, was evaluated. To assess the effect of aortic enhancement on CT image noise, image noises of excluded CT studies due to exceedingly low (< 250 HU, 221.1±22.6 HU; n=87; 80 kV, 32; 100 kV, 45; 120 kV, 10) or high (> 350 HU, 414.3± 57.1 HU; n=55; 80 kV, 46; 100 kV, 9) aortic enhancement were compared with those of the CTDI group (250–350 HU, 293.7±28.6 HU; n=177; 80 kV, 123; 100 kV, 51; 120 kV, 3).

To calculate the dose estimate of each chest CT examination, a formula used in the German pediatric CT dose survey was employed [3, 17]:

$$E = \left(\frac{DLP}{Pf}\right) \times Cf \times sC \times aC \times \left(\frac{sChead}{sCbody}\right)^x$$

where E (mSv) is the effective dose, P_f refers to the phantom factor, C_f (mSv/mGy·cm) is the effective dose normalized to the dose length product (DLP, mGy·cm), sC is the scanner correction factor in head mode (sC_{head}) or body mode (sC_{body}), aC is the patient age correction factor, and x is a factor required for scanner correction in children. The five age correction factors were applied to the corresponding five age groups: the factor for newborn to patients aged up to 1 month, the factor for 1-year-olds to patients aged between 2 months and 1 year, the factor for 5-year-olds to patients ages 2–5 years, the factor for 10-year-olds to patients ages 6–10 years, and the factor for adult to patients ages 11–15 years). To be compliant with the methods used in the German survey, a 32-cm CTDI phantom-based DLP value ($DLP_{32\ cm}$) was used to estimate the effective dose for the 11- to 15-year age group, while a 16-cm phantom-based DLP value ($DLP_{16\ cm}=DLP_{32\ cm}\times2$) was used for other age groups. The calculated CT dose estimates were compared between the two groups.

Statistical analysis was performed with a PAWS Statistics 18 for Windows (SPSS, Chicago, IL). Numerable data were described as mean±standard deviation. Between two continuous independent variables, unpaired student's t-test was used for average comparison, and Pearson's correlation coefficient was used for linear
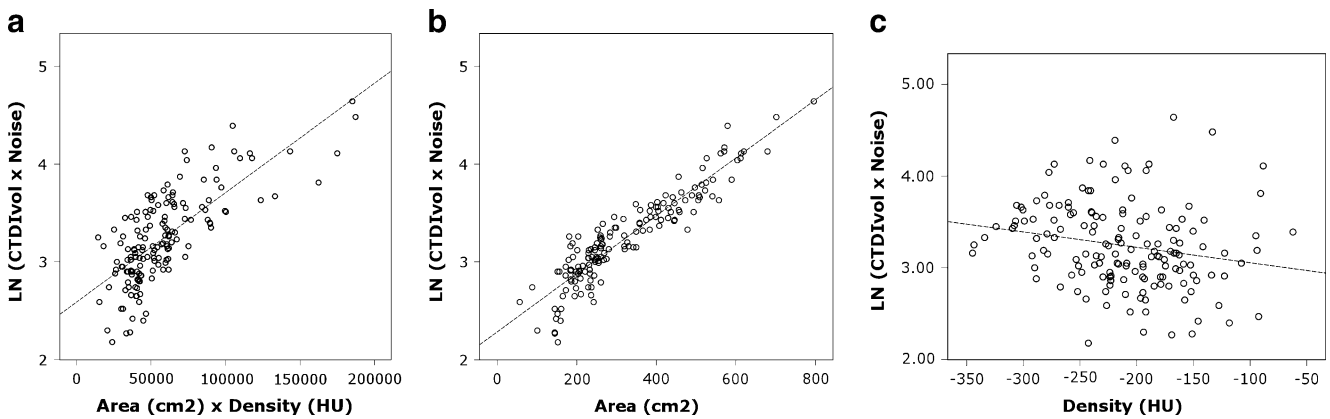
Fig. 2 Scatterplots show the correlations among the parameters in the best fit equation obtained from the pediatric chest CT examinations based on body weight. **a** A very high correlation (R^2=0.86, P<0.001) is shown between the logarithm of a product of the CTDIvol value and image noise, and a product of area and density. This best fit equation was used for the determination of individualized CTDIvol value for

pediatric chest CT in the CTDIvol group. **b** The R^2 value is also high (0.85, P<0.001) when the cross-sectional area is correlated separately with the logarithm of a product of the CTDIvol value and image noise. **c** In contrast, the R^2 value is considerably lower (0.04, P=0.01) when the density of the cross-sectional area is correlated separately with the logarithm of a product of the CTDIvol value and image noise

correlation analysis. P values<0.05 were considered statistically significant.

Results

No statistically significant difference was found in patient age (7.6±5.0 years vs. 7.9±4.9 years), aortic enhancement (287.4±42.2 HU vs. 293.7±28.6 HU), cross-sectional area (317.0±136.8 cm^2 vs. 326.3±124.8 cm^2), and mean density of the cross section (−212.9±53.1 HU vs. −221.1±56.3 HU) between the weight-based group and the CTDIvol group (P>0.05). In contrast, the CTDIvol values (based on a 32-cm CTDI phantom) displayed on the dose report after CT scanning with combined tube current modulation of the CTDIvol group (1.6±0.7 mGy), which accounted for a dose reduction of approximately 20%, were significantly lower

than those of the weight-based group (2.0±1.0 mGy) (P<0.001). The CT image noise showed no statistically significant difference between the weight-based groups (13.8±2.3 HU) and the CTDIvol group (13.6±1.7 HU) (P>0.05). On the contrary, noise differences from the target image noise of the CTDIvol group (1.1±0.9 HU) were significantly smaller than those of the weight-based group (1.8±1.4 HU) (P<0.001) (Fig. 3).

In the weight-based group, the cross-sectional area demonstrated a moderate positive correlation (γ=0.58) with the image noise at 80 kV, and the reference mAs showed moderate negative correlations (γ=−0.39, −0.46) with the image noise at both 80 and 100 kV levels (Table 3). In the CTDIvol group, the cross-sectional area showed a strong positive correlation (γ=0.73) with the image noise at 80 kV, while the mean density and reference mAs showed no and a weak negative no correlation an a with

Table 2 Cross-sectional area, kV level, and slice thickness in chest CT protocol determined by individualized volume CT dose index (n=177). Data are described by mean±standard deviation if applicable. The numbers in parenthesis in the CTDIvol column represent the range of values

Area (cm^2)	Density (HU)	Body weight (kg)	kV	Reference mAs	Reconstructed slice thickness (mm)	CTDIvol (mGy)[a]	Effective dose (mSv)	Image noise
0–199 171±24 (n=29)	−207±53	10±3	80	30±5	3.0	1.0±0.1 (0.8–1.2)	0.7±0.1	12±1
200–399 286±58 (n=94)	−233±54	24±8	80	30±6	4.0	1.3±0.2 (0.9–1.9)	0.8±0.2	14±2
400–599 468±55 (n=51)	−209±58	46±8	100	17±3	5.0	2.3±0.4 (1.8–3.6)	1.4±0.4	14±1
> 600 677±67 (n=3)	−190±70	78±7	120	16±2	5.0	4.3±1.1 (3.2–5.4)	2.4±0.6	15±1

[a] CTDIvol values were based on a 32-cm CTDI phantom. To estimate dose length product (DLP, CTDIvol × scan range [cm])-based effective dose, conversion factors derived from a 16-cm CTDI phantom were used. Therefore, CTDIvol values (e.g., 2.0 mGy) based on a 32-cm CTDI phantom were multiplied by a factor of two to obtain CTDIvol values (e.g., 4.0 mGy) based on a 16-cm CTDI phantom

Fig. 3 Scatterplots show the noise differences from the target image noise against the cross-sectional area. The noise differences are distributed more widely in the weight-based group (**a**) (1.8±1.4 HU) than the CTDIvol group (**b**) (1.1±0.9 HU) (*P*<0.001). *Dashed lines* Means of noise differences
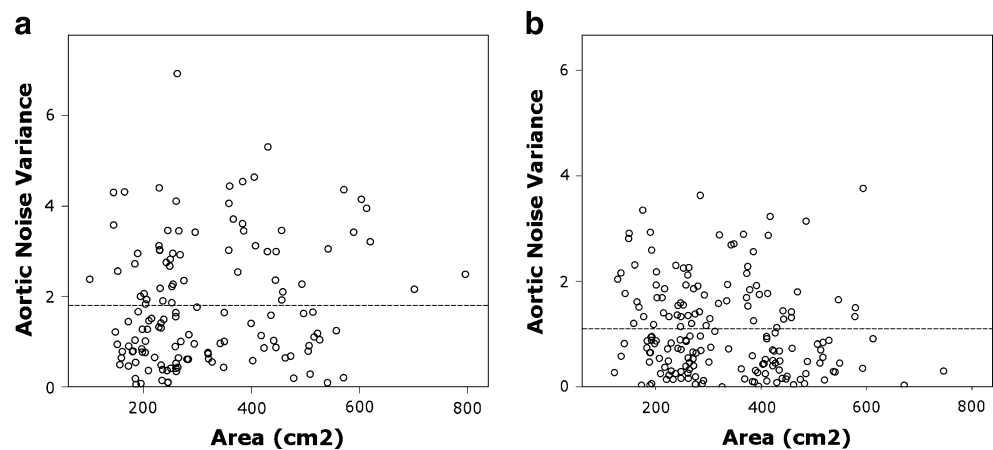
the image noise at 80 kV, respectively (Table 3). At 100 kV, the area, mean density, and reference mAs showed similarly weak positive correlations with the image noise (Table 3).

In 7.9% (14/177) of the patients of the CTDIvol group, various thoracic pathologies including consolidation or atelectasis with pleural effusion (*n*=10), cardiomegaly (*n*=2), chest mass (*n*=1), and diffuse ground glass opacities (*n*=1) were present in which the mean densities (−111.6±35.1 HU; range, −170.3 to −57.4) of the thoracic cross section were greater than those without thoracic pathologies (Fig. 1). These greater densities resulted in an increase (range, 3.2–22.1%) in CTDIvol calculated by the best fit equation of approximately 11.8±5.4%. As a rule of thumb, an increase in mean density of 1 HU accounted for an increase in the CTDIvol value of approximately 0.1%.

The CT image noise showed no statistically significant difference between the CTDIvol group (13.6±1.7) and the excluded group, due to the exceedingly low aortic enhancement (13.6±1.4), whereas, due to exceedingly high aortic enhancement, the excluded group showed significantly higher image noise (14.8±2.9) than did the CTDIvol group (*P*<0.001).

The calculated effective doses of the CTDIvol group (1.0±0.4 mSv) were significantly smaller than those of the weight-based group (1.5±0.7) (*P*<0.001) (Tables 1 and 2).

Discussion

In this study, a new protocol for contrast-enhanced pediatric chest CT was developed successfully on the basis of individualized CTDIvol values. The CTDIvol values were individually and continuously determined by the actual cross-sectional area and mean density of the body as well as the target image noise by using the best fit equation. Therefore, the measured area and mean density of the lower thoracic cross-section were the only two independent variables of each patient necessary for determining the optimal radiation dose for chest CT. This new CT protocol has four advantages over the conventional weight-based CT protocol. First, the new CT protocol provides more uniform image noise, which is supported by significantly smaller noise differences from the target noise. The result that correlation coefficients between the cross-sectional area and the image noise were higher in the new CT protocol than in the old weight-based protocol also substantiates the

Table 3 Correlation analysis of body weight, cross-sectional area, its mean density, and reference mAs with CT image noise at 80 kV and 100 kV for the two CT protocols

		Weight-based protocol		New protocol	
		Pearson correlation coefficient	*P* value	Pearson correlation coefficient	*P* value
80 kV	Area vs. noise	0.58	< 0.001	0.73	< 0.001
	Density vs. noise	0.14	0.17	−0.06	0.48
	Reference mAs vs. Noise	−0.39	<0.001	−0.20	0.026
100 kV	Area vs. noise	0.27	0.11	0.41	0.003
	Density vs. noise	0.24	0.15	0.38	0.006
	Reference mAs vs. noise	−0.46	0.005	0.42	0.002

aforementioned view (Table 3). Second, the new CT protocol offers a significantly lower radiation dose in spite of slightly greater mean area and mean density, both of which seemed to contribute to slightly higher radiation doses. These two advantages underscore the fact that the new CT protocol is better in adapting CT dose to body habitus than the weight-based CT protocol. This CT dose adaptation seemed to be attributed more to the cross-sectional area (R^2=0.85, P<0.001) and less to the mean density (R^2=0.04, P=0.01) (Fig. 2). The lack of correlation between the mean density and the image noise except at 100 kV in the new protocol also supported the result that the mean density did not contribute generally to the individualized CT dose to achieve uniform image noise (Table 3). Nevertheless, the incorporation of the mean density into the best fit equation facilitated the accomplishment of uniform image noise by slightly increasing the CT dose—an increase of approximately 0.1% in the CTDIvol value per 1 HU increase in mean density—when there were thoracic pathologic conditions increasing the mean density, such as pneumonia, atelectasis, pleural effusion, and cardiomegaly, at the same cross-sectional area (Fig. 1). Third, the new CT protocol is applicable at variable kV levels as CT dose is determined by CTDIvol rather than tube current at a fixed kV. This is crucial for contemporary pediatric body CT protocols using variable kV levels as well as variable mAs levels. Fourth, the new CT protocol is actually liberated from a CT dose table because the CTDIvol values are a continuous variable. This may reduce potential human error, i.e., inadvertent under- or overexposure, by CT technologists as a result of complicated CT dose tables in setting proper CT dose parameters. The best fit equation was incorporated into an Excel spreadsheet in a personal computer immediately next to a CT console. As a result, the new CT protocol could be successfully and rapidly adopted by CT technologists.

Tube current modulation and weight-based pediatric CT protocols have been used together [3, 4, 13]. It should be noted that the reference noise level was not fixed but adjusted to body weight in those studies. Schindera et al. [15] found that the use of a fixed reference noise level in tube current modulation resulted in higher organ doses in oversize patients. Prakash et al. [18] reported that further CT dose reduction could be achieved with weight-adjusted tube current modulation, as compared to non-weight-adjusted tube current modulation. Thus, it is clear that the reference noise level of tube current modulation should be adjusted to patient size. In fact, the reference mAs, the reference image noise index of the tube current modulation used in this study, mostly showed low, no, or irrelevant correlation with the measured image noise compared to cross-sectional area (Table 3). So far, the combined use of a CT protocol based on cross-sectional dimensions and tube

current modulation, as with the new CT protocol in this study, has not been reported. In the new CT protocol, the individualized CTDIvol value determined by the actual area and density of the lower thoracic cross-section was used to achieve an adjusted reference noise level, i.e. the target image noise. The selected noise level could then be maintained through the scanned anatomical region by means of the combined tube current modulation.

Irie et al. [11] found that the descending aorta is the optimal region in which to measure the image noise in contrast-enhanced abdominal CT because it shows homogeneous attenuation, little partial volume averaging effect as well as being located in the central portion of the body. Therefore, the image noise measured in the descending aorta in this study probably represents the image noise of each chest CT examination. To obviate a potential effect of the degree of aortic enhancement on the measured image noise, only chest CT examinations showing the aortic enhancement in the range of 250–350 HU were included in this study. Aortic enhancement below 250 HU did not affect the measured image noise but aortic enhancement above 350 HU significantly increased the measured image noise. An explanation for this interesting phenomenon is that strong aortic enhancement may increase the mean density of the thorax, which then slightly increases dose requirement as confirmed in the CTDIvol group in this study. The situation may be similar to a slight reduction of CT dose unless CT dose is adjusted as required, which then slightly increases the image noise. A recent study [19] also demonstrated that increasing contrast enhancement resulted in slightly increased image noise of abdominal CT acquired at the same noise index. Another possibility is that cardiovascular structures with strong enhancement may create some uneven beam-hardening artifacts that may contribute to a slight increase in image noise.

There were several limitations to this study. First, patient size parameters used in the new CT protocol were based on a single cross-section rather than the whole scanned thorax. However, cross-sectional dimensions and density of a patient were also obtained from a single level in other studies [4, 6–8, 10, 11]. In addition, the scan range of pediatric chest CT evaluated in this study was standardized by anatomical landmarks, which might be reflected by a single representative cross-section. Nonetheless, this approach may not be valid or may be suboptimal in other occasions in which the scan range is not standardized, and differs according to clinical indications, such as cardiac CT or focal CT. Second, three different kV levels, i.e. 80, 100, and 120 kV, were empirically determined according to the body weight in the weight-based group and according to the cross-sectional area in the CTDIvol group (Tables 1 and 2). Therefore, it is not sure whether the selected kV level was optimal. The use of low kV in contrast-enhanced pediatric

chest CT is beneficial to smaller patients because of greater dose reduction and iodine contrast. However, tube current saturation may occur in the thick regions, e.g., the shoulder, of a large patient at low kV with tube current modulation, which diminishes the dose saving effect of tube current modulation [13, 14, 18]. Now, this tube current saturation can be avoided by graphically recognizing the predicted dose curves along the z-axis prior to CT scan using appropriate software (DoseInfo; Siemens Medical Solutions). Third, variable slice thicknesses, i.e., 3.0 mm, 4.0 mm, and 5.0 mm (Tables 1 and 2), might affect image noise because image noise is inversely proportional to the square root of the reconstructed slice thickness. However, the slice thickness in pediatric CT protocols should be reduced in smaller patients in order to improve spatial resolution along the z-axis of the patient [6]. In addition, the effect of the variable slice thicknesses on image noise was present in the same amount in the two groups, probably cancelling each other out.

Regarding the best fit equation proposed in this study, it should be noted that the formula is not completely equivalent to the standard equation used in CT physics. First, image noise was included in the formula instead of the square of the image noise because inclusion of the former showed a higher correlation coefficient than inclusion of the latter (R^2, 0.86 vs. 0.53). This difference may be explained by the difference in the slice thickness (3–5 mm) and kV level (80–120 kV) used in this study, which has a considerable effect on image noise as well as on the relationship between CTDIvol and image noise. In addition to slice thickness, image noise is subject to a substantial change according to the reconstruction kernel used. Second, the cross-sectional area and its mean density were used as alternatives for body diameter and the linear attenuation coefficient in order to make the proposed formula practical for the clinical use. However, image noise variations were reduced successfully and a higher degree of CT dose adaptation to body size and habitus was achieved by using the proposed formula. Nonetheless, these modifications may be regarded as a limitation of this study and hopefully a more advanced formula will be developed.

This new individualized protocol for pediatric chest CT may also be applied to other anatomical regions such as abdomen, pelvis, head, and neck. The risk-saving effect of this approach may be greater for pediatric abdominal CT because abdominal CT typically has a greater risk of radiation exposure than chest CT. Recently, a strategy for selecting the most dose-efficient kV for CT examinations that takes into account patient size and diagnostic task was demonstrated [20]. The method presented here using cross-sectional area and its mean density of the patient used in this study may be easily and practically incorporated into this strategy as a parameter of patient size.

Conclusion

Contrast-enhanced pediatric chest CT with the CTDIvol individually determined by cross-sectional area and density of the body provides more uniform noise and better dose adaptation to body habitus than does weight-based CT at variable kV levels and with combined tube current modulation.

References

1. Kalra MK, Maher MM, Toth TL et al (2004) Strategies for CT radiation dose optimization. Radiology 230:619–628
2. Goo HW (2005) Pediatric CT: understanding of radiation dose and optimization of imaging techniques. J Korean Radiol Soc 52:1–5
3. Yang DH, Goo HW (2008) Pediatric 16-slice CT protocols: radiation dose and image quality. J Korean Radiol Soc 59:333–347
4. Singh S, Kalra MK, Moore MA et al (2009) Dose reduction and compliance with pediatric CT protocols adapted to patient size, clinical indication, and number of prior studies. Radiology 252:200–208
5. Stark G, Lonn L, Cederblad A et al (2002) A method to obtain the same levels of CT image noise for patients with various sizes, to minimize radiation dose. Br J Radiol 75:140–150
6. Boone JM, Geraphty EM, Seibert JA et al (2003) Dose reduction in pediatric CT: a rational approach. Radiology 228:352–360
7. Kalra MK, Maher MM, Prasad SR et al (2003) Correlation of patient weight and cross-sectional dimensions with subjective image quality at standard dose abdominal CT. Korean J Radiol 4:234–238
8. Jung YY, Goo HW (2008) The optimal parameter for radiation dose in pediatric low dose abdominal CT: cross-sectional dimensions versus body weight. J Korean Radiol Soc 58:169–175
9. Nyman U, Ahl TL, Kristiansson M et al (2005) Patient-circumference-adapted dose regulation in body computed tomography. A practical and flexible formula. Acta Radiol 46:396–406
10. Menke J (2005) Comparison of different body size parameters for individual dose adaptation in body CT of adults. Radiology 236:565–571
11. Irie T, Inoue H (2005) Individual modulation of the tube current-seconds to achieve similar levels of image noise in contrast-enhanced abdominal CT. AJR Am J Roentgenol 184:1514–1518
12. Hur G, Hong SW, Kim SY et al (2007) Uniform image quality achieved by tube current modulation using SD of attenuation in coronary CT angiography. AJR Am J Roentgenol 189:188–196
13. Goo HW, Suh DS (2006) Tube current reduction in pediatric non-ECG-gated heart CT by combined tube current modulation. Pediatr Radiol 36:344–351
14. Goo HW, Suh DS (2006) The influences of tube voltage and scan direction on combined tube current modulation: a phantom study. Pediatr Radiol 36:833–840
15. Schindera ST, Nelson RC, Toth TL et al (2008) Effect of patient size on radiation dose for abdominal MDCT with automatic tube current modulation: phantom study. AJR Am J Roentgenol 190: W100–W105

16. McCollough CH (2005) Automatic exposure control in CT: are we done yet? Radiology 237:755–756
17. Nagel MG, Stamm G. Paediatric CT exposure practice in the federal republic of Germany: results of a nation-wide survey in 2005/06. Hannover: Hannover Medical School. 2006. Available from URL : http://www.mh-hannover.de/fileadmin/kliniken/diagnostische_radiologie/download/Report_German_Paed-CT-Survey_2005_06.pdf
18. Prakash P, Kalra MK, Gilman MD et al (2010) Is weight-based adjustment of automatic exposure control necessary for the reduction of chest CT radiation dose? Korean J Radiol 11:46–53
19. Watanabe H, Kanematsu M, Miyoshi T et al (2010) Improvement of image quality of low radiation dose abdominal CT by increasing contrast enhancement. AJR Am J Roentgenol 195:986–992
20. Yu L, Li H, Fletcher JG et al (2010) Automatic selection of tube potential for radiation dose reduction in CT: a general strategy. Med Phys 37:234–243